

---

# Study on the impacts of urban network evolution on urban wind and heat environment based on improved genetic algorithm

Bohong Zheng<sup>1</sup>, Yanfen Zhong<sup>1,2,\*</sup>

1. College of Architecture and Art, Central South University,  
Changsha 410076, China

2. College of Civil Engineering and Architecture, Nanchang Hangkong University,  
Nanchang 320063, China

22566942@qq.com

---

**ABSTRACT.** *The irrational layout of urban space is very likely to produce urban heat island (UH). Thus, it is highly necessary to explore how the evolution and spatial distribution of urban network affect the urban wind and heat environment (W&HE). In this paper, an improved genetic algorithm (GA) is proposed to simulate the evolution of urban network, and the UH intensities (UHIs) of Changsha, China are monitored at 18 urban and 7 suburban observation points. On this basis, the author analysed the impacts of urban spatial layout on the W&HE and the UHI. The results show that: the improved GA is feasible for simulation and analysis of the evolution trend of urban network; the UH effect increased with the total urban area and building floor-area ratio (FAR); the mean daytime UHI in downtown Changsha decreased with the growth in green space ratio and increased with the growth in the hardened ground ratio. Therefore, the urban spatial layout should be planned rationally to control the development intensity, lower the ratio of hardened ground and expand the green space in the urban area. The research findings lay a solid theoretical basis for the optimal design of urban layout and the improvement of urban W&HE.*

**RÉSUMÉ.** *L'aménagement irrationnelle de l'espace urbain est très susceptible de produire un îlot urbain de chaleur. Il est donc indispensable d'explorer les effets de l'évolution et de la répartition spatiale du réseau urbain sur l'environnement urbain de vent et de chaleur. La disposition irrationnelle de l'espace urbain est très susceptible de produire un îlot urbain de chaleur (UH). Ainsi, il est très nécessaire d'étudier la façon dont l'évolution et la distribution spatiale du réseau urbain affectent l'environnement urbain de vent et de chaleur (W & HE). Dans cet article, un algorithme génétique amélioré (GA) est proposé pour simuler l'évolution du réseau urbain. Les intensités d'UH (UHIs) de Changsha, en Chine, sont surveillées à 18 points d'observation urbains et 7 suburbains. Sur cette base, l'auteur a analysé les impacts de l'aménagement spatial urbain sur le W & HE et le UHI. Les résultats montrent que: le GA amélioré est réalisable pour la simulation et l'analyse de la tendance d'évolution du réseau*

urbain; l'effet UH a augmenté avec le ratio de la zone urbaine totale et de la surface de bâtiment (FAR); la moyenne diurne UHI au centre-ville de Changsha a diminué avec la croissance du ratio d'espaces verts et a augmenté avec la croissance du ratio de terrains durcis. Par conséquent, l'aménagement de l'espace urbain devrait être planifié de manière rationnelle pour contrôler l'intensité du développement, réduire le ratio de terrain durci et élargir les espaces verts dans la zone urbaine. Les résultats de la recherche jettent une base théorique solide pour la conception optimale de l'aménagement urbain et l'amélioration du W&HE urbain.

**KEYWORDS:** urban network, urban space, wind and heat environment (W&HE), urban heat island (UH) effect, improved genetic algorithm (GA), backpropagation neural network (BPNN).

**MOTS-CLÉS:** réseau urbain, espace urbain, environnement de vent et de chaleur (W & HE), effet d'îlot urbain de chaleur (UH), algorithme génétique amélioré (GA), réseau de rétropropagation neuronale (BPNN).

DOI:10.3166/ISI.23.5.105-119 © 2018 Lavoisier

## 1. Introduction

Urban network is closely correlated with the wind and heat environment (W&HE) in that the spatial form and distribution of cities directly bear on urban microclimate (Steenefeld *et al.*, 2011, Gobakis *et al.*, 2011, Xie and Zhou, 2015). Thus, the urban microclimate and environment can be greatly improved through proper design and arrangement of urban network (Ashtiani *et al.*, 2014, Johnson, 2015).

Concerning regional distribution pattern, the urban area is thronged with tall residential and office buildings, lacking sufficient open space and green space. These buildings act like screens that block the air circulation in the downtown (Steenefeld *et al.*, 2014, Mohan *et al.*, 2013). What is worse, the heat tends to accumulate in the urban area due to the high sky cover and low sun exposure. The dense buildings, coupled with emissions of waste heat and heat absorption of cement and asphalt floors, suppress the air circulation and intensify the urban heat island (UH) effect, leading to a deteriorating W&HE (Theeuwes *et al.*, 2016, Agarwal and Tandon, 2010).

Studies have found that the distribution of urban network, including urban form, green space, water bodies and hardened ground, is a key determinant to the UH effect (Takebayashi, 2011, Zheng *et al.*, 2016). Therefore, it is very meaningful to study the correlations between the W&HE and the urban spatial layout, and, on this basis, optimize the urban network to alleviate the UH effect and improve the urban living environment (Rajagopalan *et al.*, 2014; Lee, 1979, Mochida and Lun, 2008).

The correlational analysis is often conducted using the genetic algorithm (GA) and its improved versions, especially for complex nonlinear problems (Ookaa *et al.*, 2008, Lim and Ooka, 2014). Inspired by the natural selection theory, the GA can search and collect information quickly on the global scale, i.e. encoding the optimal parameters in the search space, and prepare the optimal genetic strategy to solve complex optimization problems (Isaac *et al.*, 2008, Takebayashi *et al.*, 2011).

This paper attempts to disclose the relationship between the existing urban network layout and the urban W&HE using artificial intelligence algorithm. For this

purpose, the backpropagation neural network (BPNN) and the GA were integrated into an improved GA, and applied to explore the influence law of urban pattern evolution and spatial pattern shift on urban W&HE in Changsha, China. The research findings help to optimize urban construction and network planning (e.g. the layout of green space and water bodies in downtown), and improve urban W&HE and living comfort.

## 2. Urban space and application of improved AG

### 2.1. Urban space and the UH effect

Urban space, the spatial area “affected by urban activities”, is vertically equivalent to the atmospheric mixed layer (ML) and horizontally equivalent to the urban land area. The heat released by various urban activities accumulates within the physical boundaries of the urban space, and is diluted or discharged through urban ventilation. Urban ventilation can alleviate the UH effect and improve the urban microclimate.

The urban space is elastically changing. For a certain period of time, the urban land area does not change easily, but the ABL thickness is under constant changes. The growth in ML thickness increases the volume of urban space and promotes ventilation quality, allowing the heat within the space to dilute and diffuse. The ventilation in urban space can be regarded as the joint effect of vertical variation in ABL thickness and horizontal air flow velocity (wind speed). The quality of urban ventilation has a great impact on urban temperature.

The temperature difference between the urban area and the suburbs or rural area is known as the UH intensity (UHI), which is an important indicator of the UH effect. For an urban space, the UHI calculation formula (equation (3)) can be obtained from the mass conservation formula (equation (1)) and the UHII standard formula (equation (2)).

$$\rho c(T_u - T_r) = \frac{Q_h \cdot L \cdot S}{U \cdot MLH \cdot S} \quad (1)$$

$$UHI = T_u - T_r \quad (2)$$

$$UHI = \frac{Q_h \cdot L}{\rho \cdot c \cdot U \cdot MLH} \quad (3)$$

where  $T_u$  is the urban temperature ( $^{\circ}\text{C}$ );  $T_r$  is the suburban or rural temperature ( $^{\circ}\text{C}$ );  $c$  is the isobaric specific heat capacity of air in urban space ( $\text{J}/\text{kg}/^{\circ}\text{C}$ );  $\rho$  is the air density in urban space ( $\text{kg}/\text{m}^3$ );  $S$  is the length of the city vertical to the wind direction (m);  $Q_h$  is the intensity of heat generated in the urban space ( $\text{J}/\text{m}^2/\text{s}$ );  $MLH$  is the height of the ML in the urban space.

It can be seen from equation (3) that the UHI is not only related to the heat intensity generated in the urban space, but also to such factors as the size of the city space, the density and the specific heat capacity of the air, and the wind speed in downtown.

**2.2. Improved GA**

The GA searches for the optimal solution in a way similar to the Darwinian biological evolution. As shown in Figure 1, the traditional GA generates genetic operators by re-encoding the influencing factors, applies these operators to the original population, and yield the new population through genetic operations.

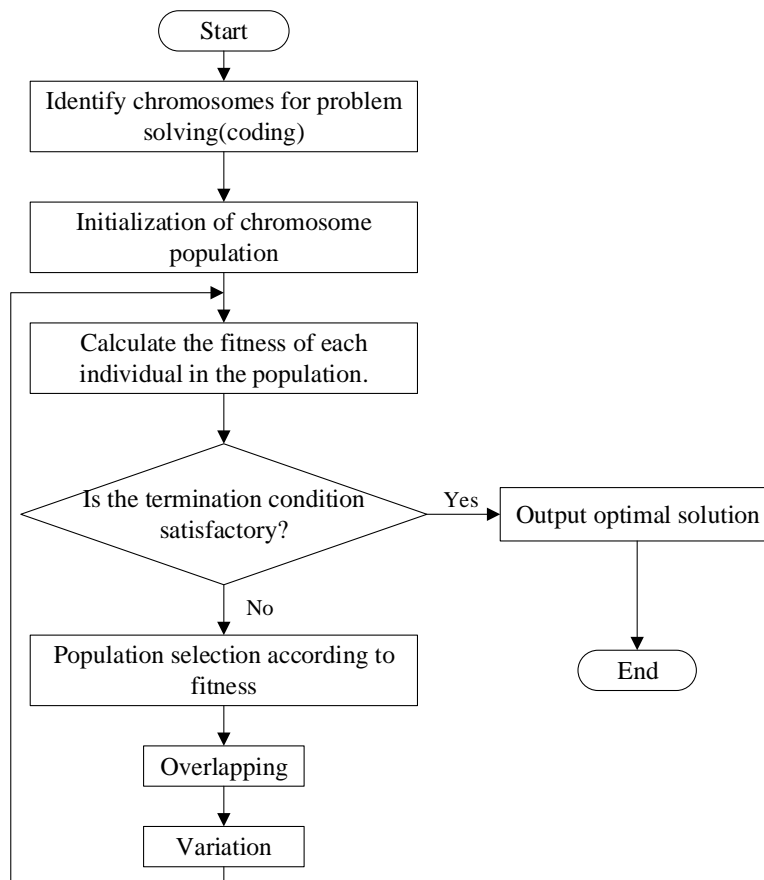


Figure 1. The flow chart of the GA

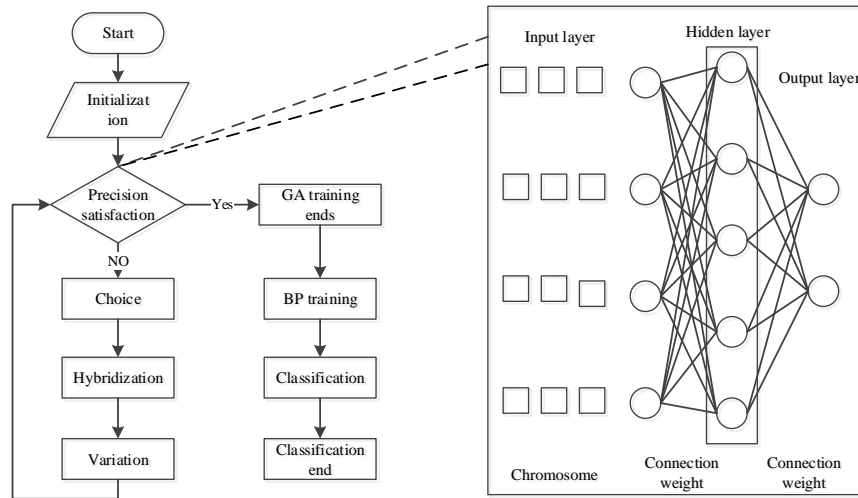


Figure 2. The flow chart of BPNN optimization by improved GA

Here, the traditional GA and the BPNN are improved by the weight optimization theory of the GA, aiming to avoid the local optimum trap in the simulation process. As shown in Figure 2, the improvement is implemented in two steps. In the first step, the parameter inputs of the BPNN were optimized by the GA, and the environmental parameters were imported to the BPNN for global search, forming a relatively optimal solution set; In the second step, the solution set was subjected to iterations till the optimal simulation result was obtained.

### 2.3. Simulation of urban network evolution based on improved GA

This paper intends to simulate the evolution of urban network in Changsha, China. The land use units of Changsha in 2015 were taken as the basic data for this research. In light of the types and distribution of land uses in 2016, random simulation points were selected from regions with obvious spatial changes. Next, the improved GA was introduced to iteratively analyse, adjust and determine the model parameters. The collected data and simulated results are displayed in Table 1 below.

As shown in the table, the improved GA adopted strict constraints during the simulation of land use rate and cover type in urban network, and the simulated results agree well with the actual values. Hence, the improved GA is a feasible and accurate prediction tool for land use type and land use rate of future cities.

Table 1. Collected data and simulated results

Year	2015		2016		2018
Surface types	Actual value	Analog value	Actual value	Analog value	Analog value
Woodland	48.19	47.65	50.71	46.51	40.31
Rivers	4.73	3.41	4.77	2.61	2.23
Building lot	10.06	11.08	11.74	11.43	14.38
Farmland	37.03	36.86	32.78	39.45	43.08

### 3. Relationship between urban form and the UH effect

#### 3.1. UHI evaluation indices

Based on the previous theoretical analysis on urban network evolution by the improved GA, this section further explores the relationship between urban form and the UH effect, aims to disclose the impacts of changing urban spatial layout on urban W&HE.

Two indices were proposed to define the aforementioned UHI, namely, the maximum UH temperature increase and the total UH temperature increase, and used to characterize the influence laws of the parameters of urban spatial layout on the UH effect. The maximum UH temperature increase refers to the difference between the maximum ambient temperature in downtown and the mean ambient temperature in the suburbs or rural area; the total UH temperature increase stands for the total heat increase in the certain urban space resulted from the UH effect. The two indices can be expressed as formulas (4) and (5) below.

$$\max \Delta T_{ij} = T_{ij} - \bar{T}_R \quad (4)$$

$$T = \frac{s \times \sum_{j=1}^m \sum_{i=1}^n x_{ij}}{10000} \quad (5)$$

where  $\Delta T_{ij}$  is the UHI at a certain spatial position  $ij$ ;  $T_{ij}$  is the surface temperature at a certain spatial position  $ij$ ;  $\bar{T}_R$  is the ambient temperature of rural area;  $T$  is the total temperature increase of the UH ( $^{\circ}\text{C h}$ );  $x_{ij}$  is the local UHI at a certain spatial position  $ij$ ;  $s$  is the size of each sub-area of the urban space.

### 3.2. Total urban is and UHI

Comparative analysis reveals that, among the various indices of urban spatial form, the total area, fractile, plaque area and dispersion are closely related to the UHI. Among them, the total area has the greatest impact to the UHI. Hence, the author probed into the relationship between the urban area and the UHI evaluation indices.

Taking Changsha as an example, the relationship curve between the total urban area and the maximum UH temperature increase is presented in Figure 3. It can be seen that, as the urban area of Changsha grew from 281km<sup>2</sup> in 2000 to 935km<sup>2</sup> in 2016, the maximum UH temperature increase in the city proper surged up from 8.6°C to 14°C.

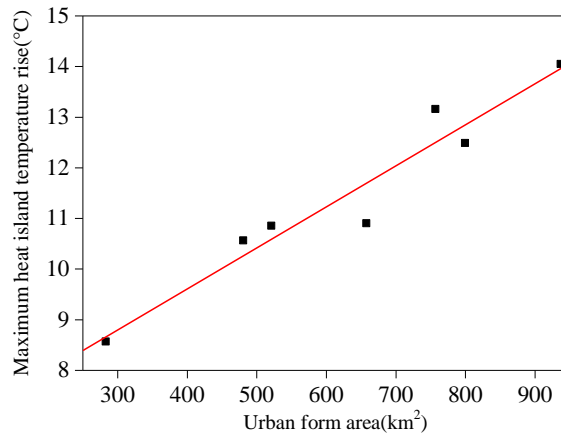


Figure 3. The relationship between the total urban area and the maximum UH temperature increase

The statistics of the total urban area and the maximum UH temperature increase was linearly fitted according to equation (6). In this way, the correlation coefficient  $R^2$  was determined as 0.934, indicating that the total urban area has a significant positive correlation with the maximum UH temperature increase. The linear fitting was proved feasible as its results passed the F-test at the significance of 0.05.

$$Y = 0.008x + 6.4 \quad (R^2 = 0.934) \quad (6)$$

The relationship curve between the total urban area and the total UH temperature increase is shown in Figure 4. Through linear regression of the statistical data, the linear relationship between the two parameters was derived (equation (7)). The relationship passes the F-test at the significance of 0.05, indicating the total urban area is positively correlated with the total UH temperature increase, that is, the total UH temperature increase grows with the expansion of the urban area. The urban temperature increase is attributable to that the growing total urban area pushes up the

energy consumed to realized urban functions, and that the amount of ventilation inside the city is suppressed by building distribution and hardened ground.

$$Y = 186x - 36050 \quad (R^2 = 0.69) \quad (7)$$

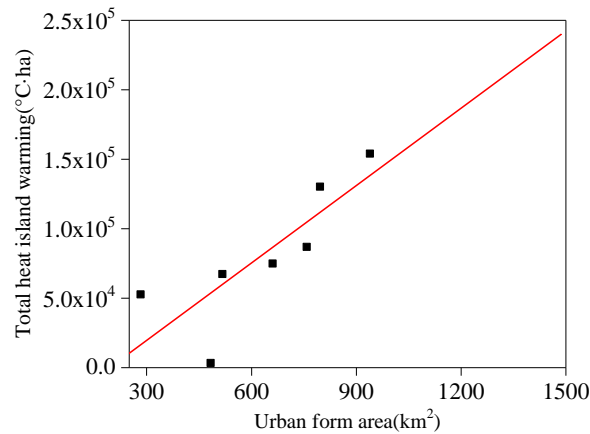


Figure 4. The relationship between the total urban area and the total UH temperature increase

#### 4. Urban network and urban W&HE

##### 4.1. Building layout and urban W&HE

The location, distance and local area of each point in the urban network have a great influence on the evaluation of the UH effect. This reflects the law of spatial correlation to a certain extent. Hence, this paper studies how the evolving spatial layouts of buildings, green space and hardened ground in urban network influence the UH effect. For our experiment, 18 observation points were selected in downtown and 7 in the suburbs. The mean temperature of the three suburban observation points with the lowest temperature was selected to compute the UHIs of the 18 urban observation points, such as to prevent the observed values from being affected by the computing uncertainties and the urbanization process.

Figure 5 presents the variations in the UHI of 2~3pm and mean daytime UHI with the floor-area ratio (FAR) at 18 urban observation points. Figure 6 shows the variations in the two parameters with building density at the same observation points. As shown in Figure 5, the UHI of 2~3pm and mean daytime UHI are positively correlated with the building FAR. It can be seen from Figure 5 that the UHI of 2~3pm is not significantly correlated with building density, while the mean daytime UHI decreased with the growth in building density.

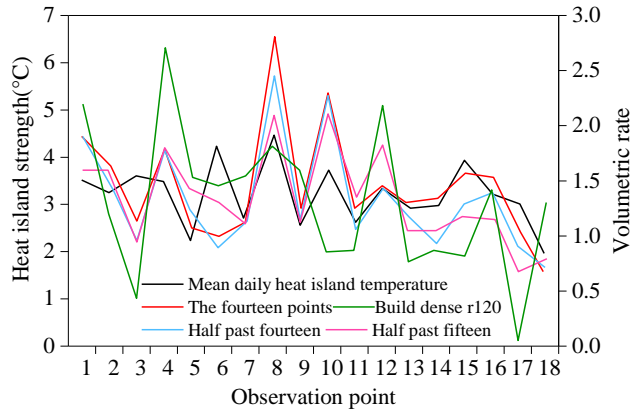


Figure 5. The variations in the UHI of 2~3pm and mean daytime UHI with the building FAR at 18 urban observation points

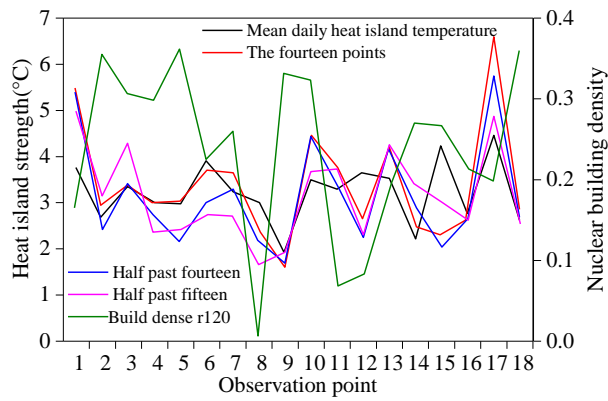


Figure 6. The variations in the UHI of 2~3pm and mean daytime UHI with building density at 18 urban observation points

In the downtown, the grid data of 1m resolution were sampled from a circular area with a radius of 120m. Then, the core building density and core building FAR were calculated using these data. After that, the correlation between urban building FAR and the UHI was described quantitatively, leading to the correlation coefficient between the two parameters. Figure 7 displays the time history of the correlation coefficient between the core building FAR and the UHI, while Figure 8 presents that between the core building density and the UHI.

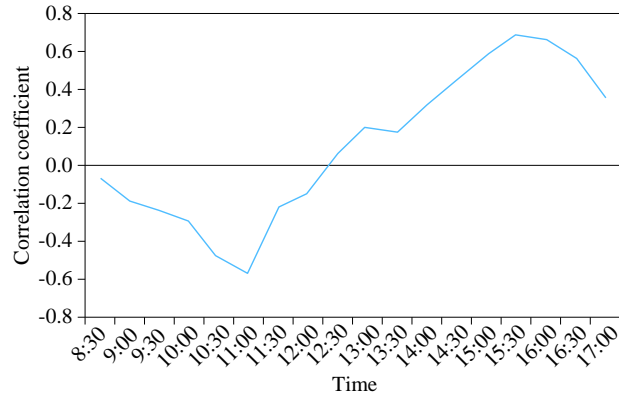


Figure 7. The time history of the correlation coefficient between the core building FAR and the UHI

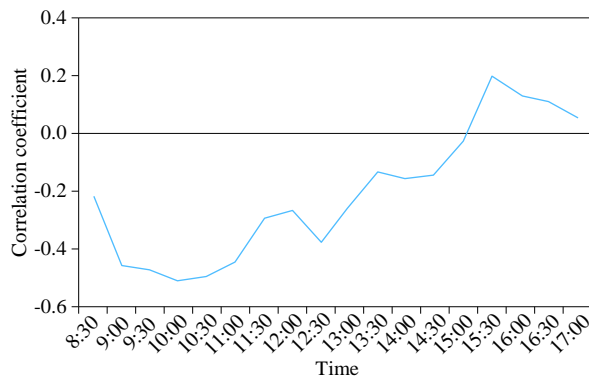


Figure 8. The time history of the correlation coefficient between the core building density and the UHI

From the two figures above, it can be inferred that the core building FAR enhanced the UH effect throughout the afternoon, pushing up the UH temperature. By contrast, the core building density is negatively correlated with the UHI, that is, the core building density lowered the UH temperature in the morning but slightly increased the latter in the afternoon. Figures 9 and 10 respectively illustrate the variations in mean daytime UHI with core building FAR and core building density, revealing that the core building FAR elevated the mean daytime UHI while the core building density had different impacts on urban heat environment at different time points.

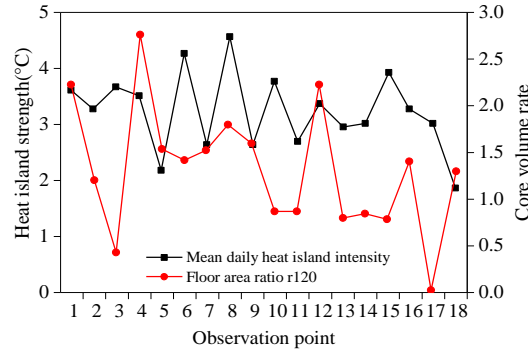


Figure 9. The variations in mean daytime UHI with core building FAR at 18 urban observation points

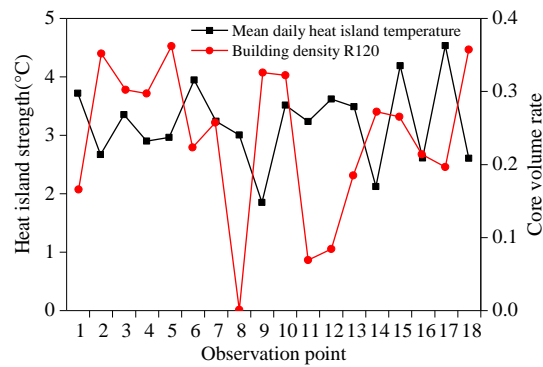


Figure 10. The variations in mean daytime UHI with core building density at 18 urban observation points

#### 4.2. Green space layout and urban W&HE

In the downtown, the grid data of 1m resolution were sampled from a circular area with a radius of 50m. Then, the core green space ratio of the circular area was calculated using these data. According to the statistical data, the trends of core green space ratio and mean daytime UHI were obtained from different observation points (Figure 11). As shown in Figure 11, the mean daytime UHI exhibited an obvious decline with the growth in the core green space ratio in the 50m-radius circle, indicating that the expansion of green space can weaken the UH effect and thus enhance the urban W&HE.

Further analysis shows that the urban ambient temperature could be adjusted by

the change in atmospheric humidity and the area of green space through reducing solar radiation and plant heat adsorption. Figure 12 shows the influence law of the change in atmospheric humidity on the correlation coefficient between green space area and the UHI. It can be seen that vegetation transpiration was inhibited when the atmosphere has a high relative humidity, which is not conducive to the cooling effect of water evaporation in vegetation.

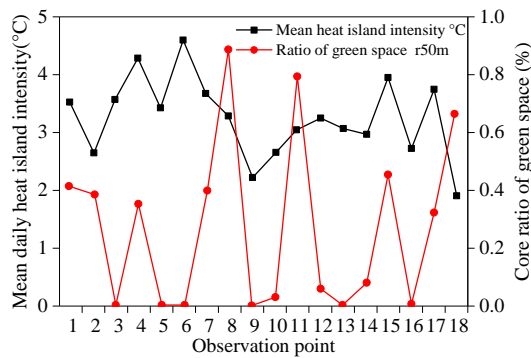


Figure 11. The trends of core green space ratio and mean daytime UHI at 18 urban observation points

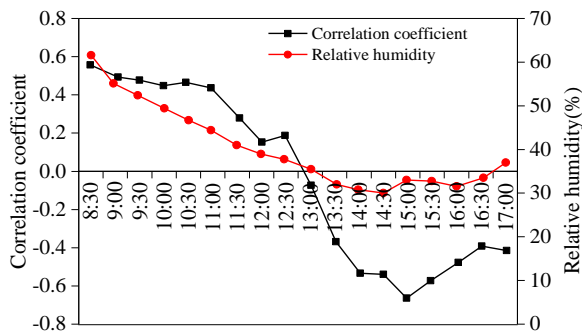


Figure 12. The influence law of the change in atmospheric humidity on the correlation coefficient between green space area and the UHI

Figure 13 shows the influence law of daytime temperature variation on the daytime cooling effect of green space. As shown in this figure, the green space’s suppression of the UH effect grew stronger before turning weaker, with the increase of daytime temperature. This is because the vegetation transpiration is strong in the morning, but grows weaker in the afternoon. Considering the significant impacts of green space area and layout on UH effect and urban W&HE, the government should protect the

existing green space, actively expand the green space in downtown, and rationally regulate the spatial layout of green space.

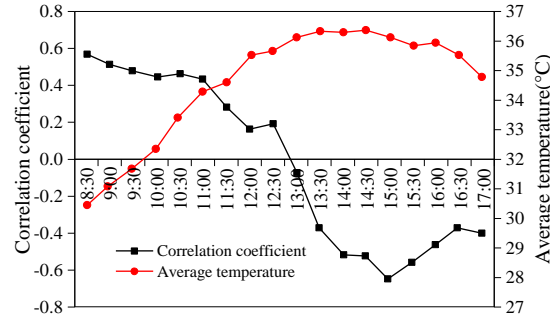


Figure 13. The influence law of daytime temperature variation on the daytime cooling effect of green space

#### 4.3. Hardened ground layout and urban W&HE

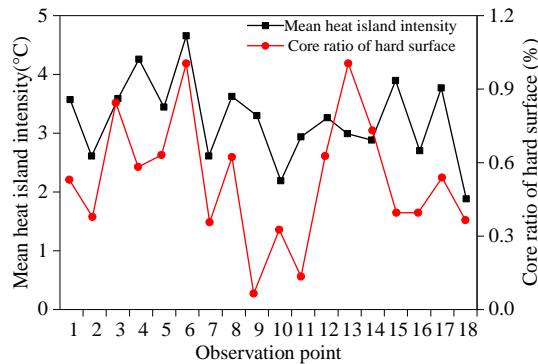


Figure 14. The trends of core hardened ground ratio and mean daytime UHI at different observation points

In the downtown, the grid data of 1m resolution were sampled from a circular area with a radius of 15m. Then, the core hardened ground ratio of the circular area was calculated using these data. After that, the trends of core hardened ground ratio and mean daytime UHI were obtained from different observation points (Figure 14). It can be seen that the core hardened ground ratio shared a similar trend with the mean daytime UHI, and the mean daytime UHI increased with the core hardened ground ratio. This means the core hardened ground ratio enhances the UH effect and hampers

the regulation of urban W&HE. Thus, the ratio of core hardened ground in downtown must be rationally planned and strictly controlled.

## 5. Conclusions

To disclose the relationship between the urban network layout and the urban W&HE, this paper proposes an improved GA, a typical artificial intelligent algorithm, and applies it to investigate how the evolution and spatial layout of urban network affect the urban W&HE. The main conclusions are as follows:

(1) The improved GA adopted strict constraints during the simulation of land use rate and cover type in urban network, and the simulated results agree well with the actual values. Hence, the improved GA is a feasible and accurate prediction tool for land use type and land use rate of future cities.

(2) The total urban area is positively correlated with the maximum UH temperature increase the growing total urban area pushes up the energy consumed to realized urban functions, and that the amount of ventilation inside the city is suppressed by building distribution and hardened ground, leading to the increase in urban temperature.

(3) The building FAR elevated the mean daytime UHI; the mean daytime UHI exhibited a sharp decline with the increase of green space ratio, indicating that the expansion of green space is conducive to improving urban W&HE; the mean daily UHI increased with the hardened ground ratio, revealing that the growth in hardened ground ratio is unfavourable to the regulation of urban W&HE.

## Reference

- Steenefeld G. J., Koopmans S., Heusinkveld B. G., Hove L. W. A. V., Holtslag A. A. M. (2011). Quantifying urban heat island effects and human comfort for cities of variable size and urban morphology in the Netherlands. *Journal of Geophysical Research Atmospheres*, Vol. 116, No. D20. <https://doi.org/10.1029/2011jd015988>
- Gobakis K., Kolokotsa D., Synnefa A., Saliari M., Giannopoulou K., and Santamouris M. (2011). Development of a model for urban heat island prediction using neural network techniques. *Sustainable Cities and Society*, Vol. 1, No. 2, pp. 104-115. <https://doi.org/10.1016/j.scs.2011.05.001>
- Xie Q., Zhou Z. (2015). Impact of urbanization on urban heat island effect based on tm imagery in wuhan, china. *Environmental Engineering & Management Journal*, Vol. 14, No. 3, pp. 647-655. <https://doi.org/10.30638/eemj.2015.072>
- Ashtiani A., Mirzaei P. A., Haghighat F. (2014). Indoor thermal condition in urban heat island: Comparison of the artificial neural network and regression methods prediction. *Energy & Buildings*, Vol. 76, No. 11, pp. 597-604. <https://doi.org/10.1016/j.enbuild.2014.03.018>
- Johnson C. (2015). Green networks: A solution to the urban heat island effect. *Sustainable City*, pp. 205-214. <https://doi.org/10.2495/sc150191>
- Steenefeld G. J., Koopmans S., Heusinkveld B. G., Theeuwes N. E. (2014). Refreshing the role of open water surfaces on mitigating the maximum urban heat island effect. *Landscape &*

*Urban Planning*, Vol. 121, No. 1, pp. 92-96.  
<https://doi.org/10.1016/j.landurbplan.2013.09.001>

- Mohan M., Kikegawa Y., Gurjar B. R., Bhati S., Kolli N. R. (2013). Assessment of urban heat island effect for different land use–land cover from micrometeorological measurements and remote sensing data for megacity delhi. *Theoretical & Applied Climatology*, Vol. 112, No. 3-4, pp. 647-658. <https://doi.org/10.1007/s00704-012-0758-z>
- Theeuwes N. E., Steeneveld G., Ronda R. J., Holtslag A. A. M. (2016). A diagnostic equation for the daily maximum urban heat island effect for cities in northwestern Europe. *International Journal of Climatology*, Vol. 37, No. 1, pp. 443-454. <https://doi.org/10.1002/joc.4717>
- Agarwal M., Tandon A. (2010). Modeling of the urban heat island in the form of mesoscale wind and of its effect on air pollution dispersal. *Applied Mathematical Modelling*, Vol. 34, No. 9, pp. 2520-2530. <https://doi.org/10.1016/j.apm.2009.11.016>
- Takebayashi H. (2011). Study on urban heat island measure effects by the wind exchange in the urban area using upper weather data. *Journal of Environmental Engineering*, Vol. 76, No. 660, pp. 195-199. <https://doi.org/10.3130/aije.76.195>
- Zheng T., Lau K. L., Ng E. (2016). Urban tree design approaches for mitigating daytime urban heat island effects in a high-density urban environment. *Energy & Buildings*, Vol. 114, pp. 265-274. <https://doi.org/10.1016/j.enbuild.2015.06.031>
- Rajagopalan P., Lim K. C., Jamei E. (2014). Urban heat island and wind flow characteristics of a tropical city. *Solar Energy*, Vol. 107, No. 9, pp. 159-170. <https://doi.org/10.1016/j.solener.2014.05.042>
- Lee D. O. (1979). The influence of atmospheric stability and the urban heat island on urban-rural wind speed differences. *Atmospheric Environment*, Vol. 13, No. 8, pp. 1175-1180. [https://doi.org/10.1016/0004-6981\(79\)90042-8](https://doi.org/10.1016/0004-6981(79)90042-8)
- Mochida A., Lun I. Y. F. (2008). Prediction of wind environment and thermal comfort at pedestrian level in urban area. *Journal of Wind Engineering & Industrial Aerodynamics*, Vol. 96, No. 10, pp. 1498-1527. <https://doi.org/10.1016/j.jweia.2008.02.033>
- Oooka R., Hong C., Katoa S. (2008). Study on optimum arrangement of trees for design of pleasant outdoor environment using multi-objective genetic algorithm and coupled simulation of convection, radiation and conduction. *Journal of Wind Engineering & Industrial Aerodynamics*, Vol. 96, No. 10, pp. 1733-1748. <https://doi.org/10.1016/j.jweia.2008.02.039>
- Lim J., Ooka R. (2014). Building arrangement optimization for urban ventilation potential using genetic algorithm and CFD simulation. *Memórias Do Instituto Oswaldo Cruz*, Vol. 102, No. 2, pp. 209-213. <https://doi.org/10.22260/isarc2014/0033>
- Isaac L., Akashi M., Kiyoshi S. (2008). Heat balance analysis for management and design of urban environment. *Hkie Transactions*, Vol. 15, No. 3, pp. 13-23. <https://doi.org/10.1080/1023697x.2008.10668120>
- Takebayashi H., Yamada T., Moriyama M. (2011). Effects of characteristics of urban block on wind environment in the street canyon. *Journal of Environmental Engineering*, Vol. 76, No. 670, pp. 1087-1092. <https://doi.org/10.3130/aije.76.1087>

